Stabilised Soil Layers Enhancing Performance of Transverse-Loaded Flexible Piles on Lightly Bonded Residual Soils

N.C. Consoli, V.P. Faro, F. Schnaid, R.B. Born

Abstract. A set of crosswise-loaded flexible piles was tested in binder stabilised top sand layers embedded in lightly bonded residual soil. Slope indicators were used to measure horizontal displacements in free-headed flexible piles during all loading stages. The geometry of the cement stabilised top sand layer surrounding the piles varied from about 2 to 4 times the pile diameter and 0.1 to 0.3 times the pile length. Experimental outcomes present an important enhancement in the performance of the flexible piles under transverse load when a cement stabilised sand layer replaces top residual soil, increasing bearing capacity and reducing maximum horizontal displacements at any given working load. At large horizontal displacements (close to failure), a linear relation is observed between the lateral load and the total lateral area compressing the natural soil around the pile. This evidence helps identifying the pile-soil interaction mechanism and provides sound normalization for test results, both considered necessary steps towards the development of a design concept for predicting lateral pile response.

Keywords: flexible piles, residual soil, top soil stabilisation, lateral load, pile field-testing.

1. Introduction

The performance of piles subjected to lateral loads is known to be mainly controlled by the properties of the soil near the surface (Simons and Menzies, 1975; Poulos and Davis, 1980; Verruijt & Kooijman, 1989; Basu *et al.*, 2009; Faro *et al*., 2015). It is for this reason that Simons and Menzies (1975) suggest being beneficial to replace poor surface soils by compacted gravel. Poulos & Davis (1980) presented an overview of methods conceived to increase the lateral resistance of piles by increasing the dimensions and/or stiffness of the piles near the ground surface. These methods comprise the use of sand or gravel fills, the insertion of wings around the pile (only near the surface), concrete collars, mortar and even short piers or beams surrounding the piles.

For analysing laterally loaded piles in a layered elastic continuum, numerical methods were used (*e.g.* Verruijt & Kooijman, 1989). Basu *et al*. (2009) supported the development of an analytic framework for assessing the response of transversally loaded piles in multi-layered elastic soils. Higgins *et al.* (2013) analysed laterally loaded pile performance using the Fourier FEM and two-layer elastic soil with constant modulus within each layer.

Field-tests in laterally loaded piles were carried out by Cintra (1981), Miguel (1996), Del Pino Jr *et al*. (2002) and Almeida *et al*. (2011) in a lateritic soil profile in order to establish values of coefficient of soil reaction. Consoli *et al.* (2016) subjected long piles to transversal load in residual soil sites and found out that lightly bonded soil might not be analysed as sedimentary fine-grained soils once the pile-soil interaction is analysed. Ferreira *et al*. (2006) and Miranda Jr. (2006) performed lateral load tests on different pile types, including omega screw piles, continuous flight auger piles, bored piles, and small diameter drilled shaft (root piles). Those tests were performed with soil in natural condition, flooded, and also with a cemented soil top layer. Conclusions pointed to a gain of approximately five times in the soil reaction coefficient due to the cemented soil layer. Rollins *et al*. (2010) performed full-scale lateral load tests on a pile group in clay before and after construction of soil mixing and jet grouting walls on either side of the pile group. According to the authors, both soil mixing and jet grouting provided significant increase in the transverse load of pile clusters. Although these results provide important insights to pile design, there is no established method to estimate the lateral load *vs.* lateral displacement response of a pile embedded in cement-treated soil and subjected to lateral load. The response ought to take into consideration the lateral resistance of the adjacent soil, especially the near-surface soil type that controls the load-displacement performance of the pile (Faro, 2014; Faro *et al*., 2015).

Nilo Cesar Consoli, Full Professor, Ph.D., Departamento de Engenharia Civil, Universidade Federal do Rio Grande do Sul, Porto Alegre, RS, Brazil. e-mail: consoli@ufrgs.br.
Vítor Pereira Faro, Associate Professor, D.Sc., Departamento de Construção Civil, Universidade Federal do Paraná, Curitiba, PR, Brazil. e-mail: vpfaro@ufpr.br.
Fernando Schnaid, Emeritus Professor, Ph.D., Departamento de Engenharia Civil, Universidade Federal do Rio Grande do Sul, Porto Alegre, RS, Brazil. e-mail: fernando@ufrgs.br.
Ricardo Bergan Born, Ph.D. Student, M.Sc., Departamento de Engenharia Civil, Universidade Federal do Rio Grande do Sul, Porto Alegre, RS, Brazil. e-mail: born@ufrgs.br.
Submitted on December 20, 2016; Final Acceptance on September 21, 2017; Discussion open until April 30, 2018.
DOI: 10.28927/SR.403219

In the present research, an attempt is made to extend these early views by interpreting results of crosswise load tests carried out in flexible piles embedded in lightly bonded residual soil with binder-stabilised top sand layers considering distinctive thicknesses and diameters around piles. Different improved top layers geometries were tested under a particular diameter-to-length ratio and, based on these results, an attempt is made to normalize data in order to help the elaboration of design methods. This follows studies of shallow foundations bearing in cement treated layers (Thomé *et al.*, 2005; Consoli *et al.*, 2008, 2009) and plate anchors subjected to pullout loads (Consoli *et al.*, 2013), as well as short rigid piles embedded in cement treated soils subjected to lateral load (Faro *et al.*, 2015).

It is important to recall that residual soils are a product of rocks *in situ* weathering. According to Leroueil & Vaughan (1990) and Blight (1990), stress history has little influence on residual soil properties since both the crystallisation associated with the formation of mother rocks and the precipitation of mineral cells create interparticle bonding. The porous cemented structure leads to distinctive geotechnical characteristics that are quite different from those of transported soils with similar densities and grain size distribution. According to Consoli *et al.* (1998), prestressing lightly bonded residual soils produces substantial damage to the cemented structure with considerable reduction in initial soil stiffness. According to the same authors, it is important to notice that the result of prestressing slightly bonded residual soils contrasts with ordinary patterns produced by overconsolidation in which soil stiffness is expected to increase along with increasing maximum past mean consolidation stress.

2. Soil Features

The present investigation reports data from transversally loaded piles in cement treated sand layers embedded in lightly bonded residual soil. Subsequently to pile execution and previously to the compaction of the cement-stabilized top sand layers, the local soil was removed according to the volumetric geometry of the cement treated soil layer to be built.

Appropriate sand-cement mixing and compaction are essential factors for the suitable performance of the pile system. For assessment between attained field compaction and laboratory referential values, field water content, density and compression strength were measured thoroughly. In overall terms, the backfill control indicated a homogenous mass with the characteristic values presented herein.

2.1. Homogeneous lightly bonded residual soil stratum

In situ cone penetration (CPT) tests were carried out to establish the main features of the studied residual soil site. Typical chart showing variations of CPT data up to 20 m depth (see Fig. 1) indicates a homogeneous residual soil stratum in which slight variations on cone tip strength

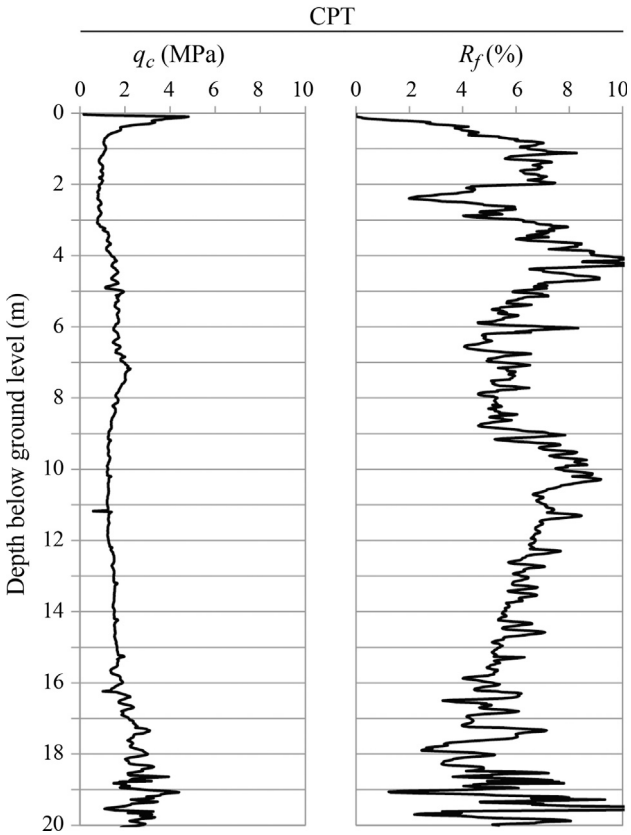

Figure 1 - CPT soil profile to a depth of 20 m.

(q_t) are attributed to weathering progression, a usual characteristic of residual soil sites. According to USCS, the residual soil was ranked as low plasticity clay (CL). The dry unit weight was around 12.1 kN/m^3 and the water table was found at about 10 m depth. Saturated drained triaxial tests were carried out in specimens collected at about 1.0 m depth and tests included measurement of strains using Hall-effect sensors (Clayton & Khatrush, 1986). Deviator stress - axial strain and volumetric strain - axial strain triaxial curves are presented in Fig. 2 considering confining stresses of 20, 60 and 100 kPa. Indication of soil bonding was obtained by testing specimens in drained triaxial compression, following experience of Consoli *et al.* (1998) in residual soil site. The stress-strain curve with smallest confining stress (20 kPa) shows high stiffness at small strains and perfectly plastic behaviour at larger strains. Increasing isotropic confining stresses from 20 kPa to 60 kPa and 100 kPa, soil stiffness is reduced at small strains due to bonding degradation (breakage of bonds) (Leroueil & Vaughan, 1990; Consoli *et al.*, 1998, 2000) and strain-hardening behaviour is observed at larger strains. Isotropic yielding occurs at a stress greater than 20 kPa and lower than 60 kPa. Volumetric strains were contractile in all studied confining stresses, increasing their maximum values with increasing confining stress. Effective friction angle of 29.5° and effective cohesion intercept of 24.0 kPa were

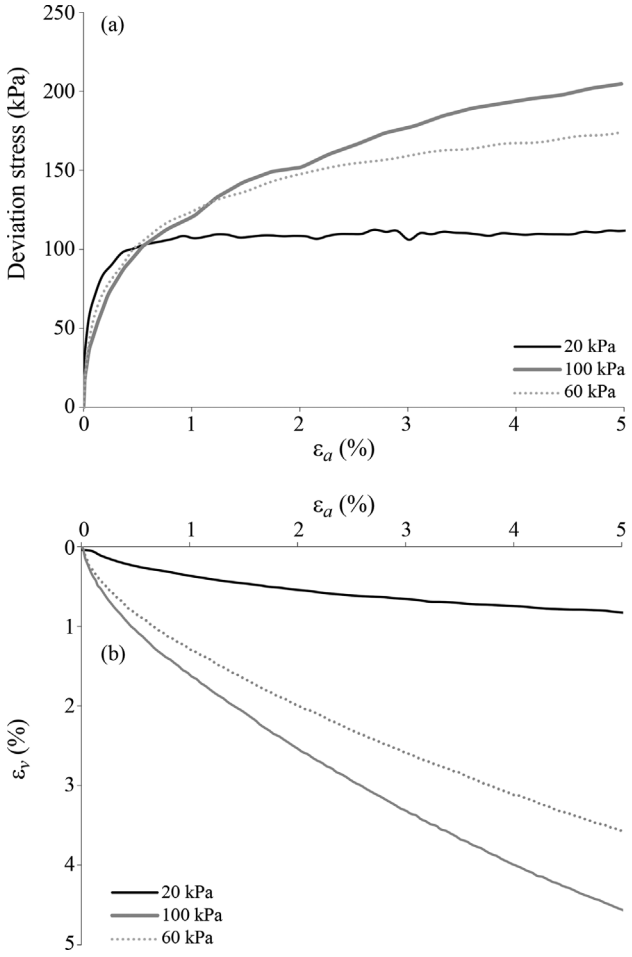

Figure 2 - Saturated drained triaxial tests of lightly bonded residual soil at confined stresses of 20, 60 and 100 kPa.

computed after triaxial test (see Fig. 3 for Mohr-Coulomb failure envelope) results. Oedometric yielding (according to Casagrande's graphical procedure) occurs at approximately 81 kPa (see Fig. 4) and unconfined compressive strength was nearly 51.2 kPa. Initial shear modulus (G_o) of about 50 MPa was determined after seismic dilatometer testing. Saturated hydraulic conductivity [obtained using a flexible wall permeameter following ASTM D 5084 (ASTM, 2016)] is relatively high at 1.5 x 10^{-5} m/s, when compared to hydraulic conductivity of alluvial clays. Different from alluvial soils with analogous particle grain sizes, residual soils are a product of *in situ* weathering, which reduces unit weight, increases hydraulic conductivity and exhibit parent rock characteristics (interparticle bonding), typical of cohesive-frictional materials.

Lastly, initial matric suction measurements carried out with the Imperial College suction probe are lower than 5 kPa, the soil does not exhibit collapse response (Medero *et al*., 2007) and therefore the lateral load-displacement response of piles in this lightly bonded residual soil is essentially dependent on the bonded structure.

2.2. Cement stabilised top sand layer

The cement stabilised top sand layer was made in a gyratory drum blender, mixing uniform fine Osorio sand previously studied by Consoli *et al.* (2010, 2011, 2012a, 2012b) and Consoli (2014), type III high early strength Portland cement (7% by weight of dry soil) and 10% water content. Strata of the sand-cement blends were constructed

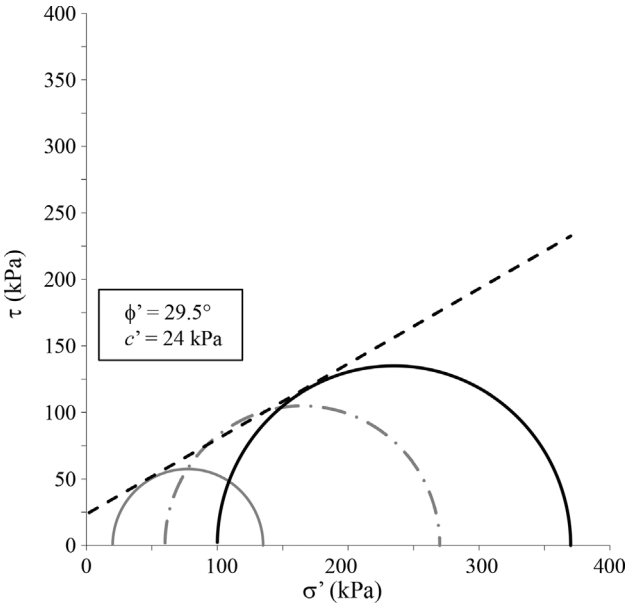

Figure 3 - Mohr-Coulomb failure envelope considering drained triaxial tests of lightly bonded residual soil at confined stresses of 20, 60 and 100 kPa.

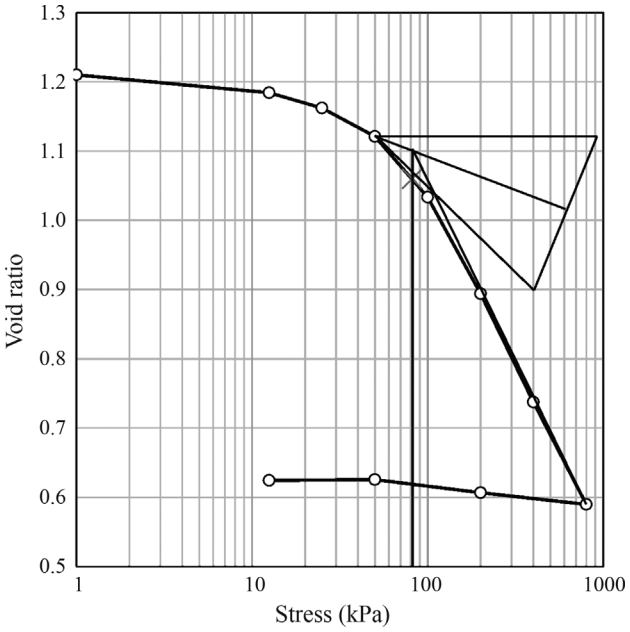

Figure 4 - Oedometric test result for lightly bonded residual soil with Casagrande's graphical procedure to obtain oedometric yield stress.

in successive sub layers, 10 cm thick each, using a vibratory plate to reach a dry unit weight of 16.0 kN/m^3. The sand-cement backfills stayed curing during 14 days previously to piles being transversally loaded. Unconfined compression tests carried out on specimens cured for 14 days produced strength of roughly 1.0 MPa. Effective cohesion intercept of 346 kPa and effective friction angle of 38.3° were determined in triaxial tests.

3. Field Testing Program

Piles were excavated with rotating auger at the experimental site portrayed above and reinforced with carbon steel tee rails 75 AS section designation (ASTM, 2010) alongside the whole length (steel tee rail used in present research in a 400-mm concrete shaft has a equivalent behaviour of a 3% - regarding shaft cross section - steel conventional cage reinforcement). Bored piles were made with concrete of uniaxial strength of about 15 MPa and transversally loaded pile tests were performed at the field testing site using 2 indistinguishable symmetrical piles in an appropriate reaction arrangement where a single pile reacts alongside another. Hence, it was concurrently feasible to have both pile reaction and test repeatability. A photo of the scheme containing the hydraulic jack horizontally positioned amid 2 steel cylinders and 2 adjusted load cells (cell capacity of 500 kN with a resolution of 2.5 kN), reacting against the top of 2 symmetrically placed piles, is presented in Fig. 5. Details of the transverse loading test schematic general plan view are shown in Fig. 6a and cross-sectional view in Fig. 6b. Most piles had a PVC pipeline in the interior to measure their horizontal displacements along the pile length during all loading stages using a slope indicator. Besides, two linear displacement transducers with resolution of 0.01 mm and 50 mm travel were used for measurement of horizontal displacements at about 100 mm above the surface of cement-stabilized sand. It is important to emphasize that close to the final stage of the gauges, they were reset at the end of the loading stage, allowing horizontal displacement measurements larger than 50 mm. Procedures for carrying out the transverse-loaded pile tests are in accord with ASTM D 3966 (ASTM, 2013). The transverse load was applied in cumulative equal increments of not

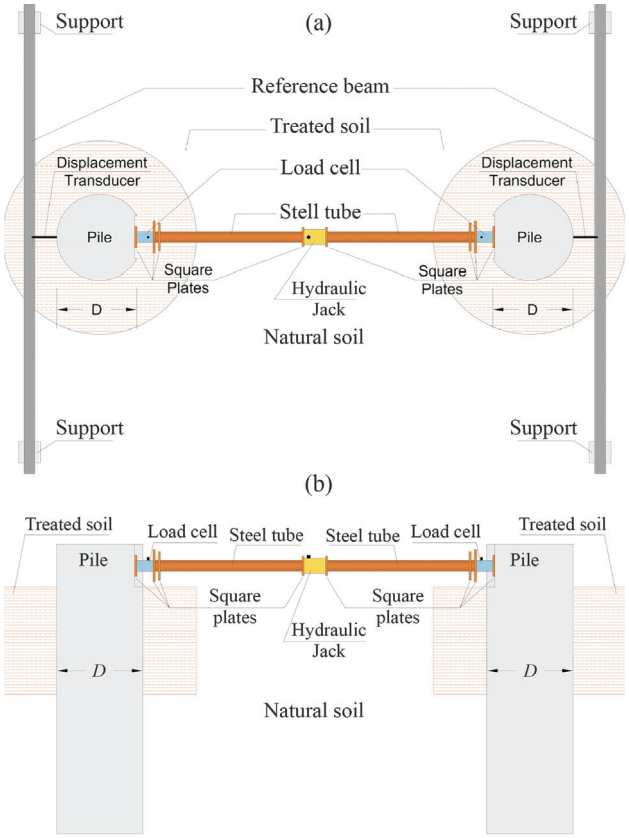

Figure 6 - Transverse loading tests schematic (a) general plan view and (b) cross-sectional view.

Figure 5 - General overview of reaction system used.

more than 1/10 of the estimated ultimate capacity. Following every transverse load increment, the required period to stabilize the displacements was expended. In agreement with Brazilian standard NBR 12131 (ABNT, 2006), every increment was sustained for at least 30 min until the following criterion [Eq. (1)] was reached:

$$L_n - L_{n-1} \leq 0.05(L_n - L_1) \quad (1)$$

where L_n is the LVDT reading at a specified time interval t, L_{n-1} the LVDT reading immediately prior to L_n, and L_1 the first reading of the stage of loading taken just following stage loading application.

Tried piles are L = 8 m long and D = 0.4 m diameter showing L/D = 20, characterising the behaviour of a free-headed flexible pile that deflects in the direction of the applied load. Besides piles inserted directly in residual soil stratum, a sequence of tests was carried out on piles embedded in cement stabilised top sand backfill layers of distinct volumes encompassing the piles. Cement stabilised top sand layers have treated diameter (D_{cem}) varying from 2 to 4 times the pile diameter (D) and treated depth (L_{cem}) varying from 0.1 to 0.3 times the pile length (L). Table 1 presents the geometry of field tests carried out on cement stabilised top sand layers. To identify each lateral load test, the following notation was used: *cem_x D_yL*, where "*cem*" denotes the top cement stabilised sand; "*x*" is D_{cem}/D *ratio* and "*y*" the L_{cem}/L *ratio.*

4. Test Results

4.1. Transverse load - displacement response

Typical horizontal load *vs.* horizontal displacements (measured 100 mm above ground by displacement transducer) of piles with stabilized backfill with dimensions corresponding to L_{cem} = 0.2L and D_{cem} = 3D and 4D are presented in Figure 7. Unloading and reloading cycles demonstrated that the system response is nonlinear elastic-plastic in all unload-reload cycles, with irrecoverable horizontal displacements clearly observed. All cycles also exhibit a strong hysteretic response.

Inclinometer probes were used for determining horizontal displacement d *vs.* depth profiles during lateral pile load tests. Since two piles are reacting against each other, two sets of results from two identical symmetrical piles were obtained, as illustrated in Fig. 8 for natural residual soil at horizontal loads corresponding to 20 kN (about elastic range), 40 kN (working load) and 60 kN (close to failure). Measured d *vs.* pile depths show very similar trends, presenting sound reproducibility at the three applied horizontal loads. Figure 9 presents an additional example for a pile embedded in treated ground (D_{cem} = 4D and L_{cem} = 0.1L) for loads of up to 260 kN. Displacements are shown to increase with increasing lateral loads to a depth of approximately 0.3 times the pile diameter; below this depth displacements are negligible. Displacements measured at

Table 1 - Specific data of each laterally loaded test and their notation.

Notation	Cement content (%)	Depth of cemented backfill [L_{cem}] (m)	Diameter of cemented backfill [D_{cem}] (m)	L_{cem}/L	D_{cem}/D	Cemented backfill volume (m^3)	Lateral load for an horizontal displacement of 25 mm at the top of the pile (kN)
Natural	-	-	-	-	-	-	50
Cem_2D_0.1L	7	0.8	0.8	0.1	2	0.30	140
Cem_3D_0.1L	7	0.8	1.2	0.1	3	0.80	155
Cem_3D_0.2L	7	1.6	1.2	0.2	3	1.61	200
Cem_4D_0.1L	7	0.8	1.6	0.1	4	1.51	255
Cem_4D_0.2L	7	1.6	1.6	0.2	4	3.02	260
Cem_4D_0.3L	7	2.4	1.6	0.3	4	4.52	300

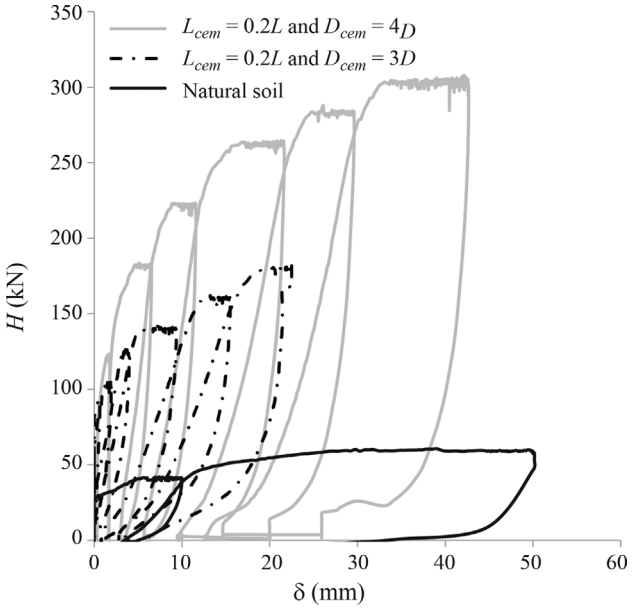

Figure 7 - Horizontal load *vs.* horizontal displacement curves for natural residual soil and cement stabilized sand backfill in different testing geometries (L_{cem} = 0.2L and D_{cem} = 3D and 4D).

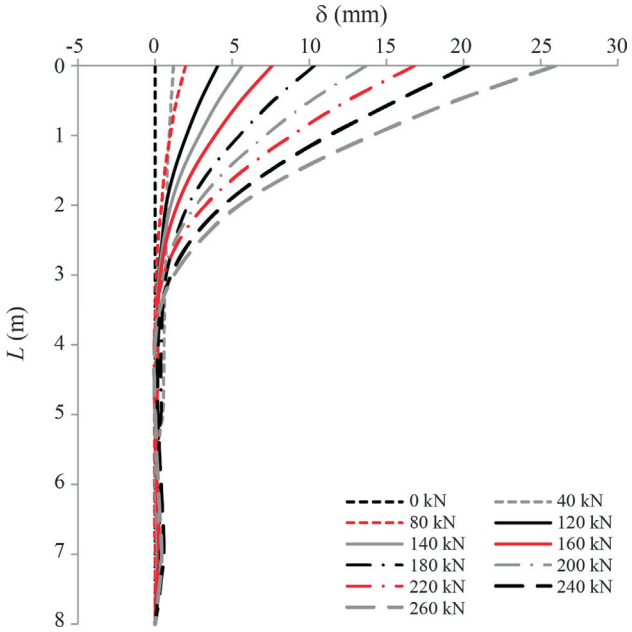

Figure 9 - Horizontal displacement *vs.* depth curves (considering horizontal loads up to 260 kN) for top cemented sand backfill with improved diameter D_{cem} = 4D and improved depth L_{cem} = 0.1L.

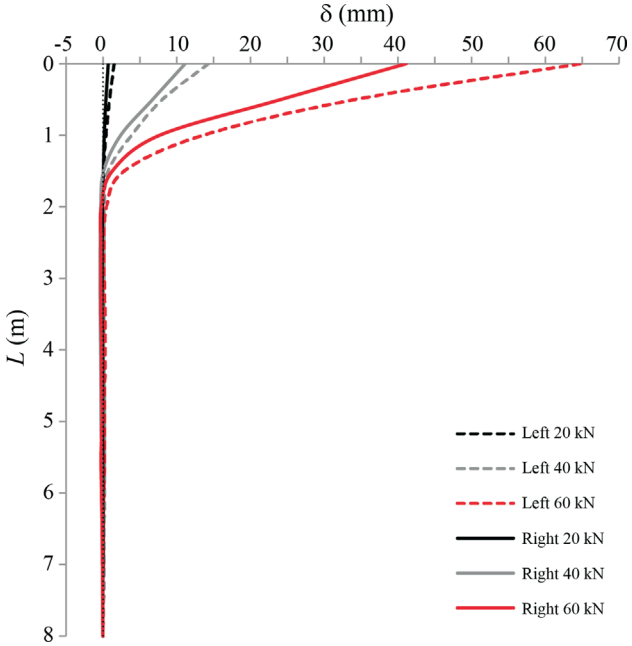

Figure 8 - Horizontal displacement *vs.* pile depth profiles (at horizontal loads of 20 kN, 40 kN and 60 kN) for two identical symmetrical piles in natural residual soil.

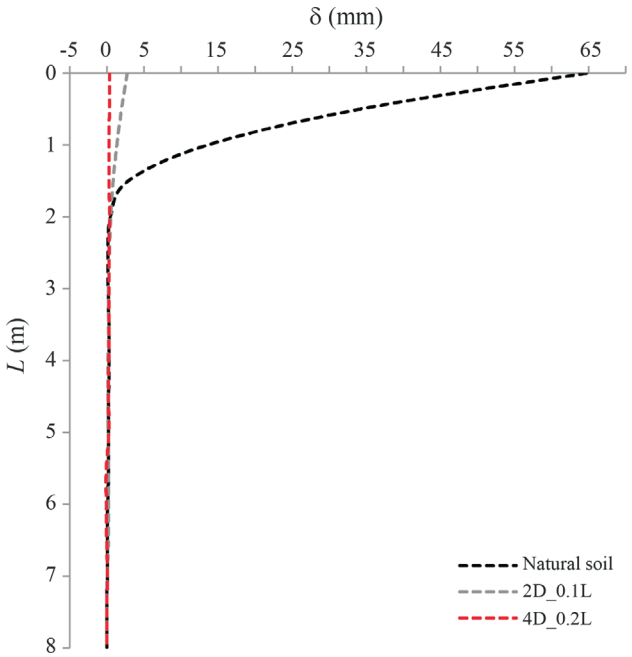

Figure 10 - Horizontal displacement *vs.* depth curves for top cemented sand backfill with distinct improved geometries considering a lateral load of 60 kN.

the surface by displacement transducers and inclinometer probe are of the same order. As an example, considering the horizontal load of 80 kN and 120 kN, the slope indicator reads 2.0 mm and 4.1 mm, while the external linear displacement reads 1.7 mm and 4.2 mm, respectively.

Figure 10 shows that, for the horizontal load of 60 kN, the pile in natural residual soil reaches an average 50 mm maximum displacement. Considering the influence of the cement stabilized improved geometry, it can be seen that, for the top cemented sand backfill with improved diameter D_{cem} = 2D and improved depth L_{cem} = 0.1L (consisting of 0.3 m^3 of cemented stabilised sand), the displacement for the horizontal load of 60 kN reduces to about 2.7 mm and,

with $D_{cem} = 4D$ and $L_{cem} = 0.2L$ (consisting of 3.0 m^3 of cemented stabilised sand - about 10 times the previous stabilised volume), a further reduction to around 0.4 mm is verified.

Figure 11 shows that, for the horizontal load of 120 kN, for the top cemented sand backfill with improved diameter $D_{cem} = 2D$ and improved depth $L_{cem} = 0.1L$ (consisting in 0.3 m^3 of cemented stabilised sand), the maximum displacement is above 10 mm, reducing to 6 mm with increasing improved diameter $D_{cem} = 3D$ and improved depth $L_{cem} = 0.2L$ (consisting in 1.6 m^3 of cemented stabilised sand). Increasing the diameter to $D_{cem} = 4D$ and reducing the improved depth to $L_{cem} = 0.1L$ (consisting in 1.5 m^3 of cemented stabilised sand), the maximum displacement reduces to 4.1 mm, further reducing to 2.6 mm with $D_{cem} = 4D$ and $L_{cem} = 0.2L$ (consisting in 3.0 m^3 of cemented stabilised sand).

5. Analysis

Before analysing results of pile lateral loading, it is important to recall that all tested piles were reinforced to yield at large load stages. The depth of the structural yield point was monitored by inclinometer measurements and was later confirmed by pile exhumation. Under this condition, maximum mobilized lateral resistance is determined as the soil reaction net of the earth pressures integrated along the pile shaft down to the critical embedment depth (*i.e.* down to the depth of yielding). Below the yield point, the piles experience virtually no lateral displacements.

A summary of the lateral load capacity of all tested piles is given in Table 1, taking the horizontal displacement of 25 mm at the top of the pile as a reference value. From measured data, it can be observed that horizontal loads increase 180% and 410%, from 50 kN to 140 kN and 255 kN, respectively, for pile in the natural soil to $D_{cem} = 2D$ and $D_{cem} = 4D$, both considering the improved depth of $L_{cem} = 0.1L$ (consisting in a volume of cemented stabilised sand increasing from 0.3 m^3 to 1.5 m^3).

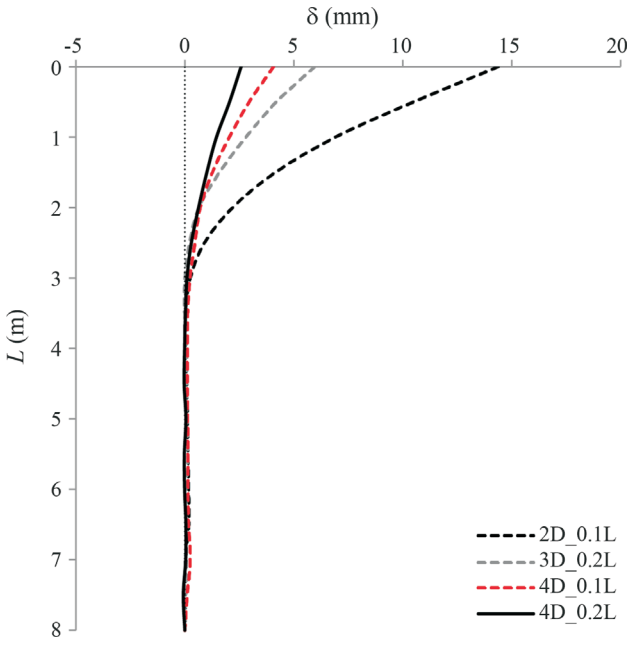

Figure 11 - Horizontal displacement *vs.* depth curves for top cemented sand backfill with distinct improved geometries considering a lateral load of 120 kN.

Figure 12 illustrates propagation of cracks in both natural ground and cemented layer when loading reaches more that 80% of transverse bearing capacity. A series of small cracks appear in the natural ground due to the compressive stress generated by the continued horizontal displacement of the cement-treated soil shaft system. It can be observed that about half the circular perimeter of the treated soil compresses the natural soil from the beginning of loading to failure and that the direction of cracks predominantly follows the direction of the pile movement.

These observed ground conditions allow an interaction mechanism to be postulated and, ultimately, a design concept to be developed. The improved ground is considered as a mass of high stiffness that moves as a solid block, compressing the less stiff natural soil (in the present study the actual stiffness of the improved ground is about 10 to 15 times that of the natural ground). It follows that ultimate bearing capacity should then be calculated as the theoretical maximum average contact pressure that can be supported without failure by the natural ground, *i.e.* the lightly structured natural ground near the surface controls the foundation horizontal resistance, since the pile and the improved ground act as one body that works in distributing the applied load only.

The second important aspect is the realization that lateral bearing capacity is not dictated by the mobilization of passive earth pressure developed at the onset of shear failure produced by pile movement, as often assumed in geotechnical design of foundations and earth structures. In lightly cemented soils, the failure model is associated to punching shear failure mechanisms which are accom-

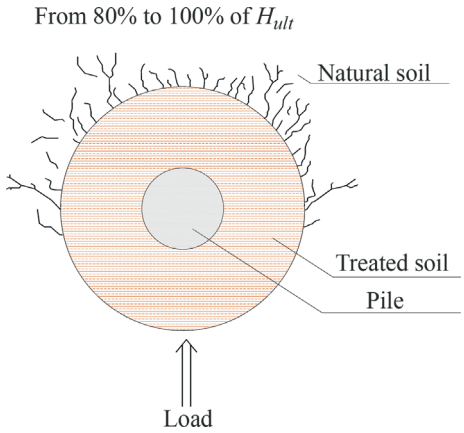

Figure 12 - Top view of failure mechanisms (cracking) on the top cement stabilized sand backfills.

plished by poorly defined shear planes, with soil zones beyond the perimeter of the loaded area being little affected. Following the basic modes of cracking displacements shown in Figure 12, the pile-soil interaction characterizes a typical punching phenomenon that comprises the origination of a series of small cracks ahead of the loaded area that, at a given applied load, exhibit brittle response and rapid fracture propagation. Pile displacements induced deformations, combined with localized volumetric strains and crack propagation, produce the breakage of the natural soil cement bonds and, at this stage, the pile reaches its maximum bearing capacity.

With the recognition that the yield stresses controlling the cemented bonds may govern the characteristic lateral bearing capacity of composite ground foundations, the results from *in situ* load tests can be further analysed. The full set of results is presented in Fig. 13, in which the lateral load ($H_{25\ mm}$) measured at the ground surface displacement of 25 mm (Table 1) is plotted against the lateral area pressing natural soil [mobilized at the pile shaft (A_{mob})] including the cemented treated superficial layer. In natural ground, A_{mob} is calculated as half the pile perimeter times the critical embedment depth (L_{crit}) of approximately 2.0 m (see horizontal displacements at Fig. 8), whereas in treated ground, A_{mob} is calculated as half the circular perimeter of the treated soil multiplied by improved depth plus half the pile perimeter times the remainder of pile length till reaching critical embedment depth (L_{crit}) (equal to 3 m in present case - see horizontal displacements in Fig. 9), which clearly define the maximum pile length mobilized by applied horizontal loads. The actual value of L_{crit} for each pile is obtained as the depth in which horizontal displacement is smaller than 0.1 mm. As observed in Fig. 13, a linear relationship ($R^2 = 0.87$) is achieved between $H_{25\ mm}$ and A_{mob}, [see Eq. (2)] including tests on piles with and without superficial ground treatment. Despite the scatter, always considered as a natural occurrence in residual soils (Schnaid & Huat 2012), there is evidence that horizontal load increases linearly with increasing mobilized area pressing natural ground.

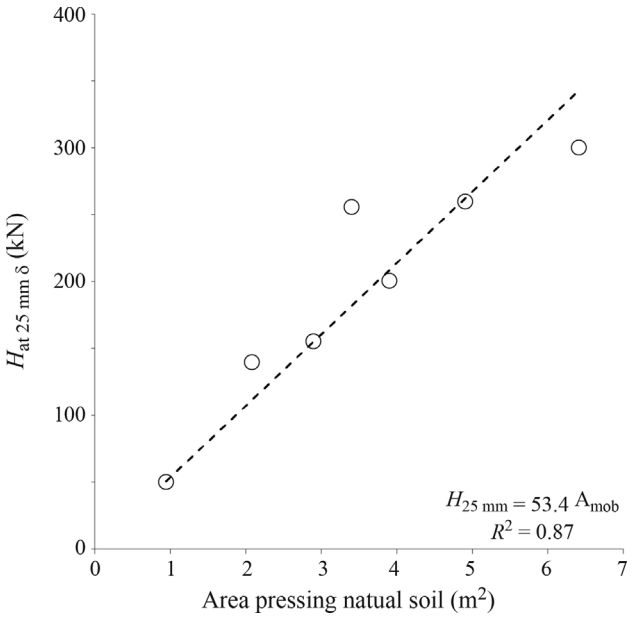

Figure 13 - Lateral loading for 25 mm horizontal displacement $H_{25\ mm}$ *vs.* area under compression (mobilized area pressing natural ground A_{mob}).

$$H_{at\ 25\ mm}\,(\mathrm{kN}) = 53.82\,A_{mob}\,(\mathrm{m}^2) \qquad (2)$$

This evidence is regarded as an indication of mobilization and mechanism associated to horizontal load transfer, which is a simple summation of pressures generated in front of both pile and cemented ground areas, despite the difference in stiffness of these materials. As a matter of fact, the constant of Eq. (2) is representative of the yielding pressure that is obtained after oedometric test, which gives an experimental evidence that the response of laterally loaded piles is actually governed by the yield stresses characterizing bond breakages in lightly cemented ground.

It is worth noticing that Consoli *et al*. (2006) have shown that there is a direct relation between isotropic yield stress and the unconfined compressive strength for lightly cemented soils. In the present case, isotropic yielding occurs at a stress greater than 20 kPa and lower than 60 kPa and the unconfined compressive strength is 51.2 kPa, both in the range of the field pressure $H_{at\ 25\ mm} / A_{mob} = 53.82$ kPa that causes failure by lateral punching. The oedometric yield stress of 81 kPa is somehow larger than the field pressure causing failure by punching. So, for practical purposes, in order to establish the maximum transverse load, the designer should request determination of the unconfined compressive strength and/or isotropic yield stress (or even oedometric yield stress) of the lightly bonded residual soil and estimate the lateral area (A_{mob}) pressing natural soil (calculated as half the circular perimeter of the treated soil multiplied by improved depth plus half the pile perimeter times the remainder of pile length till reaching critical embedment depth of long flexible piles). In a conservative first approach, A_{mob} could consider only half of the circular perimeter of the improved area times the improved depth.

6. Conclusions

Some conclusions can be drawn from the data presented in this technical paper:

- The response of transversally loaded piles is essentially governed by the yield stresses characterizing bond breakages in lightly cemented ground;
- The cement stabilised top soil layers considerably improve the behaviour of free-headed flexible piles submitted to transverse loads. The reduction of horizontal displacements under a service load is a direct function of the increase in the cement treated soil layer;

- A linear relationship is obtained between the maximum lateral load $H_{25\ mm}$ and the mobilized soil compression area (A_{mob}) ahead of the pile and the treated ground.
- In order to establish the failure transverse load, the designer should determine the unconfined compressive strength and/or isotropic yield stress (alternatively oedometric yield stress) of the lightly bonded residual soil and estimate the lateral area pressing natural soil (calculated as half the circular perimeter of the treated soil multiplied by improved depth plus half the pile perimeter times the remainder of pile length till reaching critical embedment depth of long flexible piles).

Acknowledgments

The authors desire to state their gratitude to PRONEX FAPERGS/CNPq 12/2014 (grant number 16/2551-0000469-2) and CNPq (Projects Produtividade em Pesquisa & INCT-REAGEO) for the support to the research group.

References

ABNT (2006). Piles - Static Load Test, NBR 12131, Rio de Janeiro, Brazil (in Portuguese).

Almeida, M.A., Miguel, M.G. & Teixeira, S.H.C. (2011). Horizontal bearing capacity of piles in a lateritic soil. Journal of Geotechnical and Geoenvironmental Engineering, ASCE, 137(1):59-69.

ASTM (2010). Standard Specification for Carbon Steel Tee Rails, A1-00. American Society for Testing and Materials, Philadelphia, 7 p.

ASTM (2013). Standard Test Method for Deep Foundations Under Lateral Load, D 3966, American Society for Testing and Materials, Philadelphia, 18 p.

ASTM (2016). Standard Test Methods for Measurement of Hydraulic Conductivity of Saturated Porous Materials Using a Flexible Wall Permeameter, D5084. American Society for Testing and Materials, Philadelphia, 24 p.

Basu, D.; Salgado, R. & Prezzi, M. (2009). A continuum-based model for analysis of laterally loaded piles in layered soils. Géotechnique, 59(2):127-140.

Blight, G.E. (1990). Construction in tropical soils. Proc. 2nd International Conference on Tropical Soils, v. 2, pp. 449-467.

Cintra, J.C.A. (1981). Uma Análise de Provas de Carga Lateral em Estacas e Comparação com os Métodos da Teoria de Reação Horizontal do Solo. Dissertação de Mestrado, Universidade de São Paulo.

Clayton, C.R.I. & Khatrush, S.A. (1986). A new device for measuring local axial strain on triaxial specimens. Géotechnique, 36(4):593-597.

Consoli, N.C. (2014). A method proposed for the assessment of failure envelopes of cemented sandy soils. Engineering Geology, 169:61-68.

Consoli, N.C.; Schnaid, F. & Milititsky, J. (1998). Interpretation of plate load tests on residual soil site. Journal of Geotechnical and Geoenvironmental Engineering, 124(9):857-867.

Consoli, N.C.; Rotta, G.V. & Prietto, P.D.M. (2000). Influence of cured under stress on the triaxial response of cemented soils. Géotechnique, 50(1):99-105.

Consoli, N.C.; Rotta, G.V. & Prietto, P.D.M. (2006). Yielding-compressibility-strength relationship for an artificially cemented soil cured under stress. Géotechnique, 56(1):69-72.

Consoli, N.C.; Thomé, A.; Donato, M. & Graham, J. (2008). Loading tests on compacted soil - bottom ash - carbide lime layers. Proceedings of the Institute of Civil Engineers, Geotechnical Engineering, 161(1):29-38.

Consoli, N.C.; Dalla Rosa, F. & Fonini, A. (2009). Plate load tests on cemented soil layers overlaying weaker soil. Journal of Geotechnical and Geoenvironmental Engineering, ASCE, 135(12):1846-1856.

Consoli, N.C.; Cruz, R.C.; Floss, M.F. & Festugato L. (2010). Parameters controlling tensile and compressive strength of artificially cemented sand. Journal of Geotechnical and Geoenvironmental Engineering, ASCE, 136(5):759-763.

Consoli, N.C.; Cruz, R.C. & Floss, M.F. (2011). Variables controlling strength of artificially cemented sand: influence of curing time. Journal of Materials in Civil Engineering, ASCE, 136(5):759-763.

Consoli, N. C.; Cruz, R.C.; Viana da Fonseca, A. & Coop, M.R. (2012a). Influence of cement-voids ratio on stress-dilatancy behavior of artificially cemented sand. Journal of Geotechnical and Geoenvironmental Engineering, ASCE, 138(1):100-109.

Consoli, N.C.; Cruz, R.C.; Consoli, B.S. & Maghous, S. (2012b). Failure envelope of artificially cemented sand. Géotechnique, 62(6):543-547.

Consoli, N.C.; Ruver, C.A. & Schnaid, F. (2013). Uplift performance of anchor plates embedded in cement-stabilized backfill. Journal of Geotechnical and Geoenvironmental Engineering, ASCE, 139(3):511-517.

Consoli, N.C.; Faro, V.P.; Schnaid, F.; Maghous, S. & Born, R.B. (2016). Crosswise-loaded pile tests on residual soil site. Géotechnique Letters, 6(3):216-220.

Del Pino Jr, A.; Segantini, A.A.S. & Carvalho, D. (2002). Análise de estacas escavadas carregadas transversalmente, em solo colapsível, com umidade natural e após sua inundação. XII COBRAMSEG, São Paulo, ABMS, v. 3, pp. 1493-1501.

Faro, V.P. (2014). Lateral Loading in Deep Foundations Associated to Cement Treated Soil Layers: Conception, Load Tests and Design Guidelines. Ph.D. Thesis, Federal University of Rio Grande do Sul, Brazil (in Portuguese).

Faro, V.P.; Consoli, N.C.; Schnaid, F.; Thomé, A. & Lopes Jr., L.S. (2015). Field tests on laterally loaded rigid piles in cement treated soils. Journal of Geotechnical and Geoenvironmental Engineering, 141(6):06015003.

Ferreira, C.V.; Lobo, A.S.; Albiero, J.H.; Carvalho, D. & Albuquerque, P.J.R. (2006). Comportamento de estaca carregada lateralmente, implantada em solo reforçado com solo-cimento. Proc. X Congresso Nacional de Geotecnia, Portugal, pp. 1089-1098.

Higgins, W.; Vasquez, C.; Basu, D. & Griffiths, D.V. (2013). Elastic solutions for laterally loaded piles. Journal of Geotechnical and Geoenvironmental Engineering, ASCE, 139(7):1096-1103.

Leroueil, S. and Vaughan, P.R. (1990). The general and congruent effects of structure in natural soils and weak rocks. Géotechnique, 40(3):467-488.

Medero, G.M.; Schnaid, F. & Gehling, W.Y.Y. (2007). Oedometer behavior of an artificial cemented highly collapsible soil. Journal of Geotechnical and Geoenvironmental Engineering, 134(1):9-15.

Miranda Jr., G. (2006). Estacas Submetidas a Esforços Horizontais em Solos Colapsáveis do Interior de São Paulo, nas Condições Natural, Melhorada e Inundada. Tese de Doutorado, Universidade Estadual de Campinas, p. 303.

Miguel, M.G. (1996). Execução e Análise de Provas de Carga Horizontal em Estacas em Solo Colapsível. Dissertação de Mestrado, Escola de Engenharia de São Carlos, Universidade de São Paulo, p. 162.

Poulos, H.G. & Davis, E. (1980). Pile Foundations Analysis and Design. John Wiley & Sons Inc., New York, p. 397.

Rollins, K.M.; Herbst, M.; Adsero, M. & Brown, D. (2010). Jet-grouting and soil mixing for increased lateral pile group resistance. Proceedings GeoFlorida 2010: Advances in Analysis, Modeling & Design, ASCE, Orlando, Florida, pp. 1563-1572.

Schnaid, F. & Huat, B.B.K. (2012). Sampling and testing of tropical residual soils. In: Handbook of Tropical Residual Soils Engineering. CRC Press, London, pp. 65-112.

Simons, N.E. & Menzies, B.K. (1975). A Short Course in Foundation Engineering. Newnes-Butterworths, London, p. 159.

Thomé, A.; Donato, M.; Consoli, N.C. & Graham, J. (2005). Circular footings on a cemented layer above weak foundation soil. Canadian Geotechnical Journal, 42(6):1569-1584.

Verruijt, A. & Kooijman, A.P. (1989). Laterally loaded piles in a layered elastic medium. Géotechnique, 39(1) 39-49.

List of Symbols

A_{mob}: Area under compression mobilized at the pile shaft
D: Diameter of pile
D_{cem}: Diameter of cement treated layer
G_o: Initial shear modulus
H: Horizontal load
$H_{25\ mm}$: Horizontal load at a top displacement of 25 mm
L: Length of pile
L_{cem}: Thickness of cement treated layer
L_{crit}: Critical embedment depth
L_n: LVDT reading at a specified time interval t
L_{n-1}: LVDT reading immediately previous to L_n
L_1: First LVDT taken just after loading application
δ: Horizontal displacement